Taylor & Francis
Taylor & Francis Group

RESEARCH PAPER

🔓 OPEN ACCESS ✔ Check for updates

Association of cell death mechanisms and fibrosis in visceral white adipose tissue with pathological alterations in the liver of morbidly obese patients with NAFLD

Anna-Sophia Leven [ID]a,b, Robert K. Gieseler [ID]a,c, Martin Schlattjan [ID]d, Thomas Schreiter [ID]a,c, Marco Niedergethmann [ID]b, Theodor Baars [ID]a,e, Hideo A. Baba [ID]d, Mustafa K. Özçürümez [ID]a,f, Jan-Peter Sowa [ID]a,c,#, and Ali Canbay [ID]a,g,#

aDepartment of Medicine, University Hospital, Knappschaftskrankenhaus Bochum, Ruhr University Bochum, Bochum, Germany; bGeneral and Visceral Surgery, Alfried Krupp Hospital Ruettenscheid, Essen, Germany; cLaboratory of Immunology & Molecular Biology, University Hospital, Knappschaftskrankenhaus Bochum, Ruhr University Bochum, Bochum, Germany; dInstitute for Pathology, University Hospital, University of Duisburg-Essen, Essen, Germany; eSection of Metabolic and Preventive Medicine, University Hospital, Knappschaftskrankenhaus Bochum, Ruhr University Bochum, Bochum, Germany; fDepartment of Laboratory Medicine, University Hospital, Knappschaftskrankenhaus Bochum, Ruhr University Bochum, Bochum, Germany; gSection of Hepatology and Gastroenterology, University Hospital, Knappschaftskrankenhaus Bochum, Ruhr University Bochum, Bochum, Germany

ABSTRACT

The role of visceral white adipose tissue (vWAT) in the progression of non-alcoholic liver disease (NAFLD) with its sub entities non-alcoholic fatty liver and steatohepatitis (NAFL; NASH) is underinvestigated. We thus explored mechanisms of fibrosis and regulated cell death in vWAT and liver tissue. In NAFLD, women displayed significantly more fibrosis in vWAT than men, and collagen 1α mRNA expression was significantly upregulated. The degrees of fibrosis in vWAT and liver tissue correlated significantly. The size of vWAT-resident adipocytes in NAFLD correlated negatively with the local degree of fibrosis. The extent of apoptosis, as measured by circulating M30, positively correlated with the degree of fibrosis in vWAT; necrosis-associated HMGB1 mRNA expression was significantly downregulated in vWAT and liver tissue; (iii) necroptosis-related RIPK-3 mRNA expression was significantly upregulated in vWAT; and autophagy-related LC3 mRNA expression was significantly downregulated in vWAT, while upregulated in the liver. Thus, the different cell death mechanisms in the vWAT in NAFLD are regulated independently while not ruling out their interaction. Fibrosis in vWAT may be associated with reduced adipocyte size and thus partially protective against NAFLD progression.

Abbreviations: ATG5: autophagy related 5; BAS: bariatric surgery; BMI: body mass index; ELISA: enzyme-linked immunosorbent assay; EtOH: ethanol; FFAs: free fatty acids; HCC: hepatocellular carcinoma; HMGB1: high-mobility group box 1 protein; IHC: immunohistochemistry; IL: interleukin; LC3: microtubule-associated proteins 1A/1B light chain 3B; M30: neoepitope K18Asp396-NE displayed on the caspase-cleaved keratin 18 fragment; M65: epitope present on both caspase-cleaved and intact keratin 18; NAFL: non-alcoholic fatty liver; NAFLD: non-alcoholic fatty liver disease; NAS: NAFLD activity score; NASH: non-alcoholic steatohepatitis; NLRP3: nucleotide-binding oligomerization domain, leucine-rich repeat and pyrin domain containing 3; qRT-PCR: quantitative real-time polymerase-chain reaction; r: Pearson's correlation coefficient (r); r_s: Spearman's rank correlation coefficient; RIPK3: receptor-interacting serine/threonine-protein kinase 3; T2DM: type 2 diabetes mellitus (T2DM); TUNEL: terminal deoxynucleotidyl transferase-mediated dUTP nick-end labelling; vWAT: visceral WAT; WAT: white adipose tissue

Introduction

Recent studies estimate the global prevalence of non-alcoholic fatty liver disease (NAFLD) at ~25% (10–40%) of the adult population, and it is the most common liver disease in children and adolescents in developed countries [1]. Thus, non-alcoholic fatty liver (NAFL) and its inflammatory progressive form, non-

---

alcoholic steatohepatitis (NASH), are becoming the leading cause of liver-related morbidity and mortality, with NASH being a primary indication for liver transplantation [1–4]. Excess fat accumulation in hepatocytes is found in NAFL, and NASH is characterized by additional portal and lobular inflammation, plus hepatocyte injury. A subset of patients develops fibrosis, which can progress to cirrhosis. Also, hepatocellular carcinoma (HCC) and cardiovascular complications are co-morbidities of NAFL and NASH [5,6]. Obesity and the metabolic syndrome are common underlying factors of NAFLD, which is closely associated with insulin resistance. Genetic and epigenetic factors might explain interindividual variations in disease phenotype, severity, and progression. To date, no effective medical interventions exist that completely reverse the disease other than lifestyle changes, dietary alterations and, possibly, bariatric surgery (BAS). However, several strategies that target pathophysiological processes such as an oversupply of fatty acids to the liver, cell injury, and inflammation are currently under investigation. NAFLD can be detected by ultrasonographic or MRI imaging, but NASH can only be diagnosed by liver biopsy/histology as the gold standard. Thus, non-invasive strategies are being evaluated to replace or complement biopsies, especially for follow-up monitoring [3,7].

Fibrosis in general is associated with repetitive tissue injury, chronic inflammation, and repair. It is generally considered an end-stage condition causing organ dys- and malfunction that eventually leads to the organ's demise as seen in liver, kidney, pulmonary, and cardiac diseases [8–10]. In NAFLD, liver fibrosis is characterized by the accumulation of extracellular matrix components (including collagen) and indicates disease progression [8,11]. Although the complete pathophysiology of NAFLD is still ill-defined, it is the hepatic manifestation of the metabolic syndrome as defined by morbid obesity, hypertension, dyslipidemia, and raised blood glucose [12–15]. The metabolic syndrome develops due to insulin resistance, the altered release of lipids and free fatty acids (FFAs) from adipocytes, and the chronic subcutaneous inflammation of white adipose tissue [16,17]. Therefore, visceral white adipose tissue (vWAT) might play a similarly important role in the development and progression of NAFLD [18,19]. Still, it remains unknown whether vWAT contributes to the development of liver fibrosis [18–21]. We thus investigated whether vWAT in morbid obesity exhibits fibrosis and if vWAT fibrosis may be associated with NASH or liver fibrosis in NAFLD. Adiponectin is an adipokine with reduced concentrations in obesity [22,23]. We investigated if adiponectin concentrations might be affected by vWAT fibrosis, as circulating adiponectin levels rise during the development of liver fibrosis [24].

Since the interaction between different types of cell death might be essential in the pathogenesis and progression of NAFLD [25], we also examined a potential association between cell death in vWAT and the occurrence of fibrosis. In particular, we investigated the magnitude and correlations of regulated cell death mechanisms (apoptosis, necrosis, necroptosis, pyroptosis, and autophagy-dependent cell death) [26] in vWAT and liver tissue in NAFLD. Identifiers applied by us were (i) the neo-epitope M30 exposed upon caspase 3-dependent cleavage of cytokeratin 18 for apoptosis [27]; (ii) the mRNA expression of high-mobility group box 1 protein (HMGB1) for necrosis [28]; (iii) the receptor-interacting serine/threonine-protein kinase 3 (RIPK3) for necroptosis (a hybrid mechanism of apoptosis and necrosis) [29–31]; (iv) the inflammasome NOD-, LRR- and pyrin domain-containing protein 3 (NLRP3) for pyroptosis, which triggers the production and release of the pro-inflammatory cytokines interleukin (IL)-1β and IL-18 [32]; and (v) for autophagy-dependent cell death, the expression of microtubule-associated proteins 1A/1B light chain 3B (LC3) [33] as the most prominent marker of autophagosomes [34], the autophagy related 5 (ATG5) protein [35], and Beclin-1 [36].

Results

In NAFLD, collagen 1a mRNA expression is significantly upregulated in vWAT, and collagen deposition in vWAT and liver tissue is correlated

In a cohort of 84 morbidly obese patients with NAFLD (63 females; 21 males/age range: 46–84 years) with vWAT and liver tissue available, we analysed associations of fibrosis and cell death processes in both tissues. Basic and demographic data of the patient cohort can be found in Table 1.

In morbidly obese patients with NAFLD, a larger area of vWAT was Sirius Red positive compared to controls, indicating more vWAT fibrosis in patients with NAFLD (Figure 1(a-c)). Fibrosis in vWAT was generally more prominent in older patients than in younger individuals (Figure 1(d)). Interestingly, the extent of fibrosis was inversely correlated with the BMI (Figure 1(e)). Women were more frequently affected by fibrosis in vWAT than men (Figure 1(f)). However, we found no sex-related difference in the expression of collagen 1α mRNA in vWAT (Figure 1 (g)). The extent of fibrosis in vWAT did not differ

Table 1. Demographical and clinical characteristics of the patient cohort.

Parameters	Total population	Women	Men	Reference values
Sample size [n]	84	63	21	–
Age [years (range)]	44.17 (24–66)	43.70 (24–66)	45.45 (31–63)	–
BMI [kg/m^2]^a	51.92 ± 8.62	51.90 ± 8.58	52.07 ± 8.99	18–26
NAS [median (range)]	3 [1–7]	3 [1–7]	3 [1–7]	–
NAFL/NASH	63 (75.0%)/19 (22.6%)	35 (55.5%)/26 (41%)	13 (62%)/8 (38.0%)	–
Adipocyte diameter [μm]^a	132.29 ± 21.98	131.48 ± 21.82	134.72 ± 22.91	–
AST [U/l]^a	28.61 ± 12.30	28.05 ± 13.34	30.18 ± 8.89	<35
ALT [U/l]^a	34.58 ± 19.26	32.61 ± 18.46	40.05 ± 20.77	<35
γ-GT [U/l]^a	40.12 ± 30.58	35.57 ± 24.07	52.73 ± 42.07	<35
Creatinine [mg/dl]^a	0.79 ± 0.30	0.75 ± 0.32	0.90 ± 0.21	0.6–1.1
Total cholesterol [mg/dl]^a	203.00 ± 37.72	205.9 ± 36.32	195 ± 41.39	<200
LDL [mg/dl]^a	134.78 ± 33.52	137.0 ± 32.85	128.50 ± 35.46	<160
HDL [mg/dl]^a	48.01 ± 12.82	49.36 ± 12.09	44.10 ± 14.32	>40
FBG [mg/dl]^a	104.07 ± 51.42	105.9 ± 56.53	98.85 ± 33.88	74–99
HbA1c [%]^a	6.02 ± 1,63	5.96 ± 1,72	6.15 ± 1.38	<5.7
Quick value [%]	97.52 ± 5.40	98.35 ± 5.91	97.50 ± 3.80	70–130

AST aspartate aminotransferase, ALT alanine aminotransferase, BMI body mass index, FBG fasting blood glucose, γ-GT glutamyl transferase, HbA1c haemoglobin A1c, HDL high-density lipoprotein, LDL high-density lipoprotein, NAS NAFLD activity score, NAFL Non-alcoholic fatty liver (defined as NAS ≤ 4), NASH Non-alcoholic steatohepatitis (defined as NAS > 4), SD standard deviation.
^{a}Mean ± SD.

between patients with NAFL and NASH (Figure 1(h)). Nevertheless, NASH patients exhibited a higher expression of collagen 1α mRNA in vWAT than patients with NAFL (Figure 1(i)). T

The expression of collagen 1α mRNA was significantly upregulated in the vWAT of patients *vs.* controls (Figure 1(j)), while its expression in the patients' liver tissue was slightly lower than in the controls (Figure 1(k)). The expression of collagen 1α mRNA and the extent of fibrosis in vWAT showed no correlation (Figure 1(l)). Finally, the amount of fibrosis in vWAT and liver tissue from the same patients showed a significant positive correlation (Figure 1(m)).

In NAFLD, the size of vWAT-resident adipocytes negatively correlates with extent of fibrosis in vWAT, and serum adiponectin levels are significantly downregulated in NASH

Concentrations of circulating adiponectin did not significantly correlate with the degree of fibrosis in vWAT (Figure 2(a)), while the adipocyte diameters negatively correlated with collagen deposition in this tissue (Figure 2(b)). When adipocytes in vWAT were grouped according to diameters of ≤125 μm *vs.* >125 μm, there was a statistically significant difference between the extent of fibrosis in patients with smaller *vs.* larger vWAT-resident fat cells (Figure 2(c)). Thus, the results in Figures 2(b-c) jointly confirm that the presence of hypertrophic adipocytes in vWAT is associated with a lower degree of collagen deposition in this tissue. There was no difference between patients with smaller and larger adipocytes in the systemic adiponectin concentrations (Figure 2(d)). However, serum adiponectin levels were significantly downregulated in patients with NASH as opposed to those with NAFL (Figure 2(e)).

In NAFLD, the extent of apoptosis and fibrosis are correlated in vWAT

We found a positive correlation between serum M30 (surrogate marker for apoptosis) and the degree of fibrosis in vWAT. In contrast, no correlation was found between M65 (overall cell death marker) and vWAT fibrosis (Figure 3(a-b)). No correlations were observed between M30 or M65 and collagen deposition in liver tissue (Supplementary Figure 1 **A, B**). There was no difference between patients with NAFL and NASH in serum M30, while NASH patients displayed significantly higher M65 serum levels than NAFL patients (Figure 3(c-d)). There was no difference in serum levels of M30 and M65 or number of TUNEL-positive cells in vWAT between women and men (Figure 3(e-g)). No significant correlation was found between the numbers of TUNEL-positive cells and the degree of fibrosis (Figure 3(h)). Representative photomicrographs of TUNEL-positive cells in vWAT of NAFLD patients are shown in Figure 3(i-j).

In NAFLD, necrosis-associated HMGB1 mRNA expression is significantly downregulated in vWAT and liver tissue

HMGB1 transcription was significantly downregulated in liver tissue and vWAT of patients with NAFLD compared to controls (Figure 4(a-b)). No difference in HMGB1 mRNA expression was observed between patients with NAFL and NASH in vWAT or liver tissue (Figure 4(c-d)). mRNA expression of HMGB1 was not correlated between vWAT and liver tissue (Figure 4(e)). Regarding the mRNA expression of HMGB1 and collagen 1α mRNA expression or the amount of collagen deposition in vWAT (by Sirius Red), respectively, we found no significant correlations (Figure 4(f-g)).
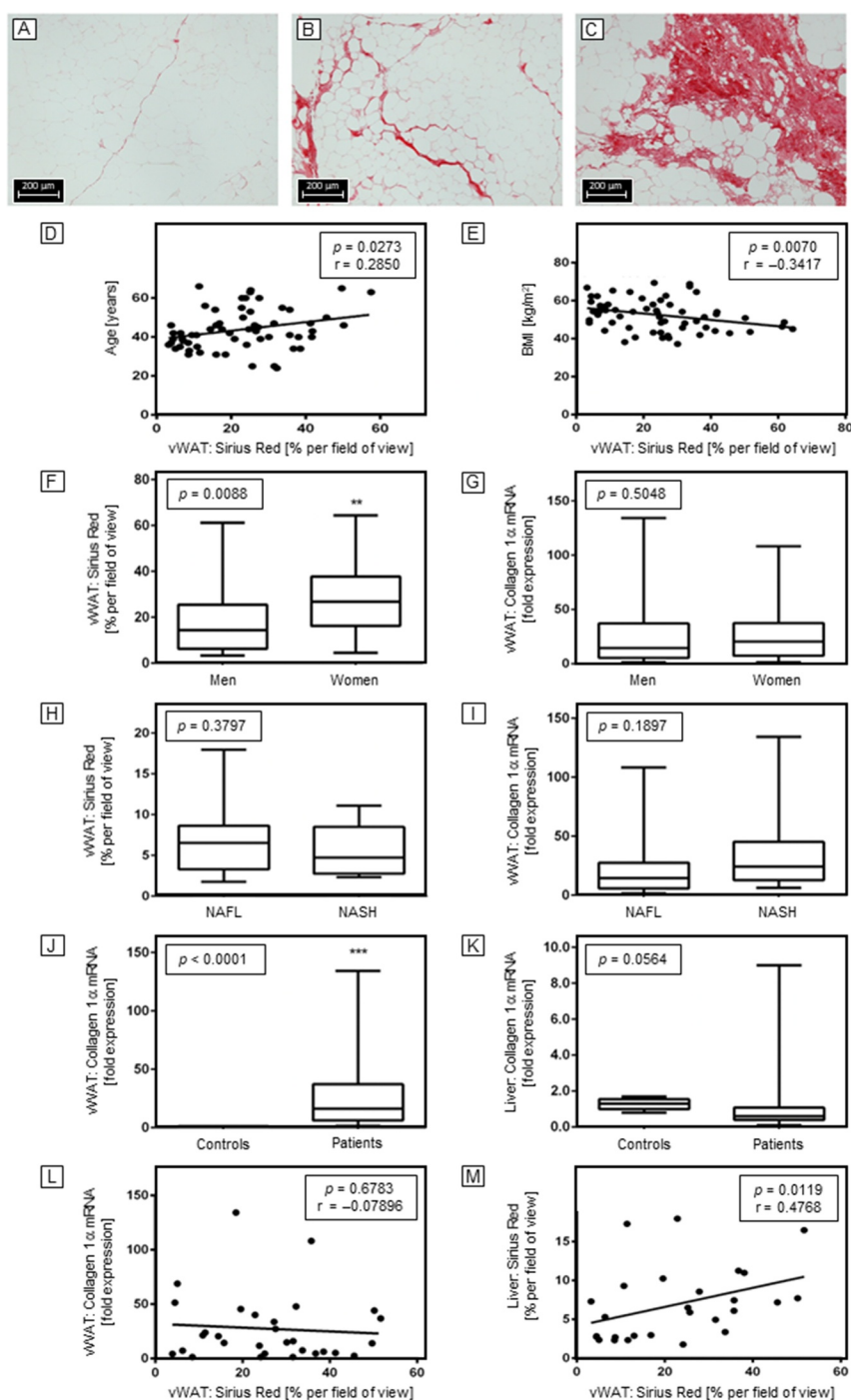
Figure 1. Fibrosis and collagen 1α mRNA expression in vWAT or liver tissue. A–C Sirius Red staining for collagen within vWAT of patients who underwent bariatric surgery. Shown are representative photomicrographs of collagen deposition in vWAT samples obtained from three different patients (magnification: x10 by light microscopy, and see the μm bars). Quantification was performed for n = 4 fields of view per 67 samples. **D** The age of the patients correlated positively with the extent of fibrosis in vWAT (n = 59). **E** In contrast, the BMI correlated negatively with fibrosis (n = 58). **F** A significantly greater extent of fibrosis was found in vWAT of women compared to men. **G** However, no differences in collagen 1α mRNA expression were detected in the vWAT of female and male NAFLD patients. **H, I** The amount of collagen deposition (h) and collagen 1α mRNA expression (i) did not differ in vWAT of patients with NAFL and NASH. **J** Collagen 1α mRNA expression was significantly upregulated in the vWAT of patients compared to controls. **K** In contrast, collagen 1α mRNA expression was lower in the patients' liver tissue compared to controls. **L** In vWAT, collagen 1α mRNA expression and the degree of fibrosis were not correlated (n = 30). **M** The degree of fibrosis in vWAT and liver tissue of NAFLD patients correlated significantly (n = 26). Statistics: *: $p \geq 0.01$ to 0.05; **: $p \geq 0.001$ to 0.01; ***: $p < 0.001$/r: Pearson's correlation coefficient.

Figure 2. Fibrosis in vWAT is inversely correlated to adipocyte size. A Adiponectin serum levels were not correlated with the extent of vWAT fibrosis (n = 28). **B** The adipocytes' diameters were significantly inversely correlated with vWAT fibrosis (n = 47). **C** In vWAT, significan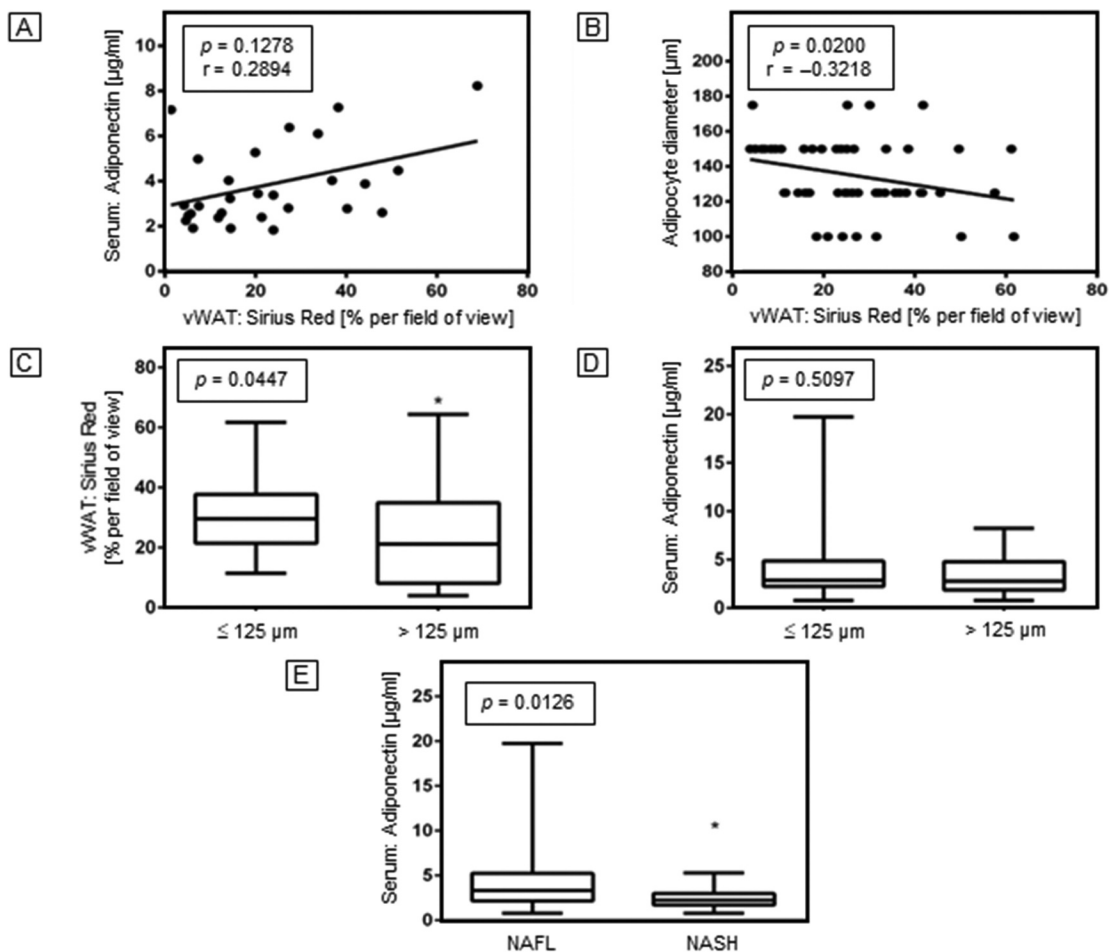tly less fibrosis occurred in the presence of larger adipocytes. **D** Adiponectin concentrations were not significantly different between patients with small or large adipocytes' diameters. **E** We identified significantly lower adiponectin concentrations in NASH patients when compared to patients with NAFL. Statistics: *: $p \geq 0.01$ to 0.05; **: $p \geq 0.001$ to 0.01; ***: $p < 0.001$/r: Pearson's correlation coefficient.

In NAFLD, RIPK-3 mRNA expression is significantly upregulated in vWAT, and is correlated to circulating IL-18

We found significantly upregulated mRNA expression of RIPK3 in vWAT in NAFLD patients compared to controls (Figure 5(a)). There was no significant correlation of RIPK3 mRNA expression in vWAT with the extent of fibrosis in vWAT (Figure 5(b)).

As RIPK3 and NLRP3 interact in inflammasome activation, we quantified the expression of NLRP3 mRNA in vWAT and liver tissue of patients with NAFLD (Figure 5c, d). In vWAT there was no significantly different NLRP3 expression between patients with NAFLD and controls (Figure 5c), though a much broader interindividual variance in NAFLD was

observed. In liver tissue, expression of NLRP3 mRNA was significantly reduced in patients with NAFLD compared to controls (Figure 5d). We next determined the expression of IL-18 mRNA downstream of possible NLRP3 activation. Both in vWAT and liver tissue, there was a much greater interindividual variance of IL-18 mRNA expression in NAFLD patients, but no difference between controls and patients (Figure 5e, f). We also measured associated serum levels of pro-IL-1β, IL-1β, and IL-18 (Figure 5g-k). While serum IL-18 levels did not differ between patients and controls (not shown), vWAT RIPK3 mRNA expression and serum IL-18 concentrations were significantly correlated (Figure 5i). Pro-IL-1β and IL-1β serum concentrations were detectable in 27 (pro-IL-1β) and 11 (IL-1β) patients. IL-1β serum concentrations were correlated to liver mRNA expression of IL-1β and serum
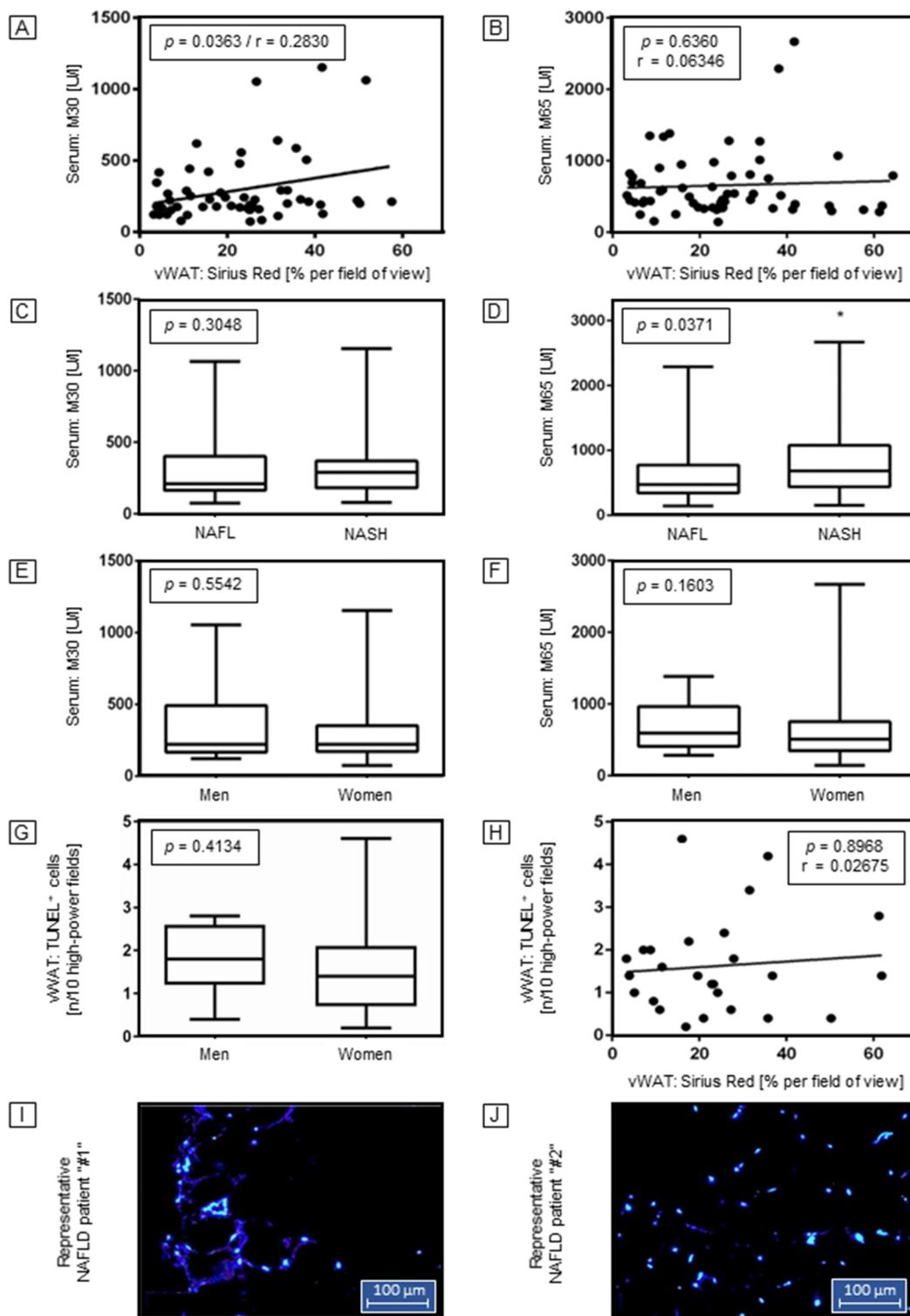
Figure 3. Serum M30 concentrations but not M65 concentrations are correlated to vWAT collagen deposition. A–B Correlation of cell death serum markers M30 and M65 to fibrosis in vWAT (n = 67). **A** We found a significantly positive correlation between M30 (indicating apoptosis only) and the degree of fibrosis (n = 54). **B** In contrast, M65 (covering both apoptosis and necrosis) did not correlate with fibrosis (n = 56). **C–F** Cell death markers M30 and M65 in the sera of patients with NAFL *vs.* NASH, and in male *vs.* female patients with NAFLD. **C** M30 did not differ significantly between NAFL and NASH. **D** In contrast, M65 was significantly higher in NASH than in NAFL, which indicates elevated non-apoptotic cell death in NASH when compared to NAFL. Neither the levels of M30 (e) nor those of M65 (f) showed significant sex-specific differences. **G** The number of TUNEL-positive cells did not differ significantly between men and women. **H** No significant correlation was found between TUNEL-positive cells and fibrosis (n = 25). **I** and **J** Representative photomicrographs of TUNEL-positive cells (green) in paraffin vWAT sections of NAFLD patients (arbitrarily designated '#1' and '#2') by fluorescence microscopy. Nuclei were counterstained with DAPI (blue). Magnification: x20. Statistics: *: $p \geq 0.01$ to 0.05; **: $p \geq 0.001$ to 0.01; ***: $p < 0.001$/r: Pearson's correlation coefficient.
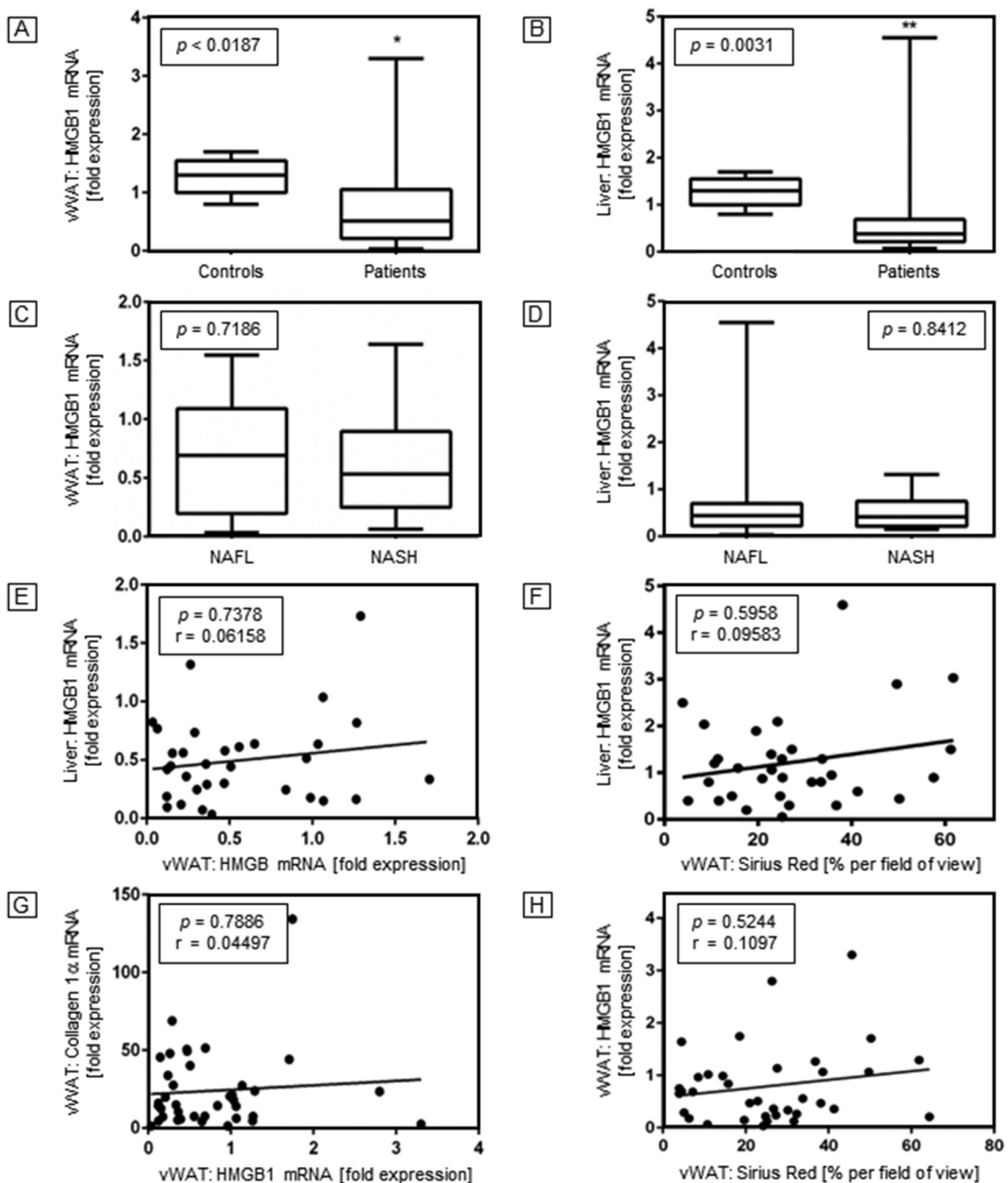
Figure 4. HMGB1-expression in vWAT and liver tissue of NAFLD is reduced. A–D HMGB1 mRNA expression in vWAT and liver tissue of NAFLD patients compared to controls, and differentiated between NAFL and NASH. **A** and **B** Compared to the controls, HMGB1 mRNA expression was significantly downregulated in both vWAT and liver tissue of NAFLD patients. **C** and **D** HMGB1 mRNA expression was not statistically significantly different in vWAT or liver of patients with NASH *vs*. NAFL. **E–H** No significant correlations between HMGB1 mRNA expression and expression of collagen 1α mRNA expression or collagen deposition in vWAT and liver of NAFLD patients were observed (**E**: n = 39; **F**: n = 33; **G**: n = 33; **H**: n = 36). Statistics: *: $p \geq 0.01$ to 0.05; **: $p \geq 0.001$ to 0.01; ***: $p < 0.001$. r: Pearson's correlation coefficient.
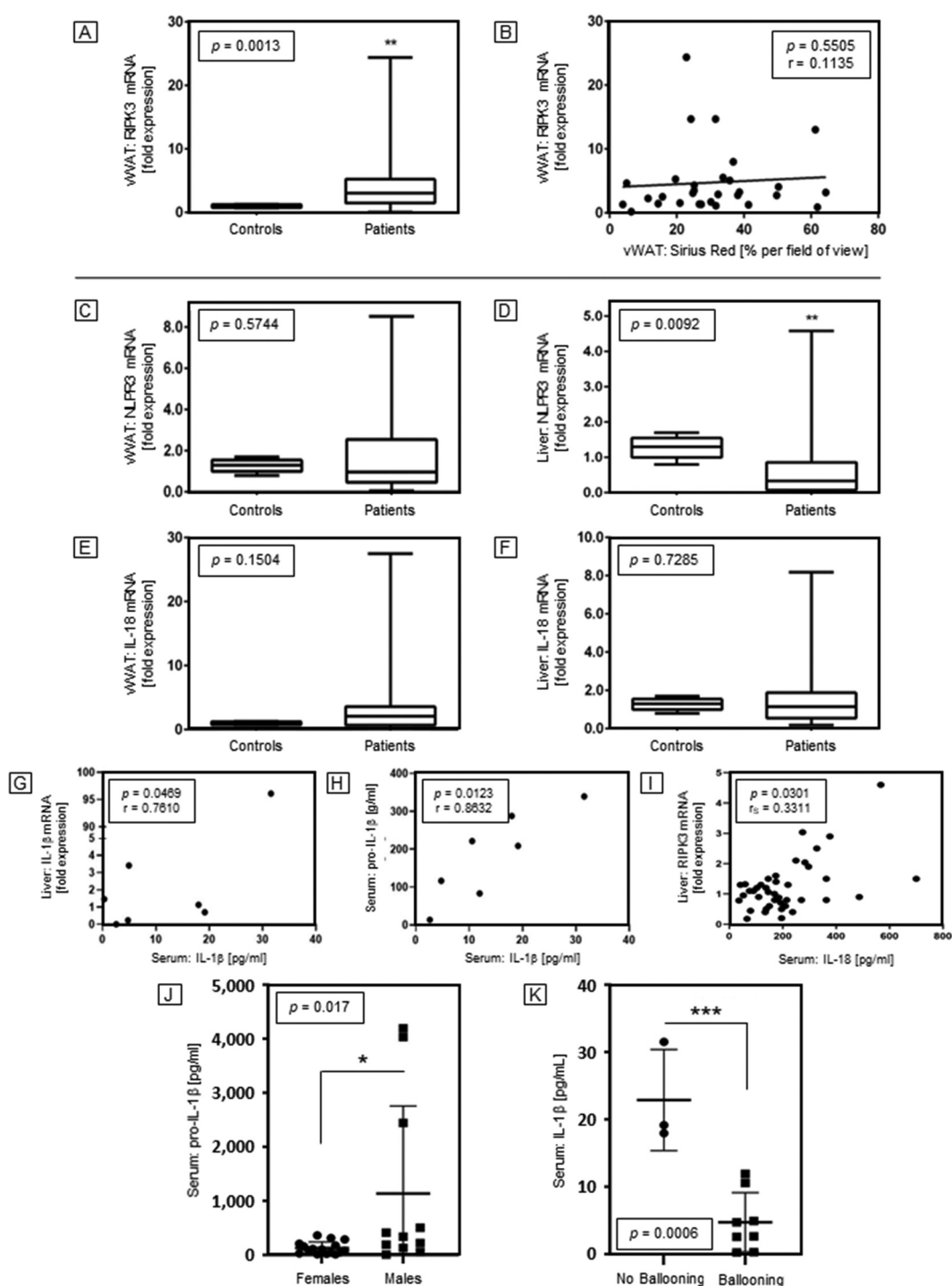
**Figure 5. RIPK3 expression is increased in vWAT and NLRP3 expression is decreased in liver tissue of patients with NAFLD.**
A–B Necroptosis: RIPK3 mRNA expression in vWAT of NAFLD patients *vs.* controls, and RIPK3 mRNA correlation with collagen deposition in vWAT of NAFLD patients. **A** In vWAT of NAFLD patients, RIPK3 mRNA expression was significantly upregulated compared to the controls. **B** The expression of RIPK3 mRNA did not correlate with collagen deposition in the patients' vWAT (n = 31). **C–F** Pyroptosis: NLRP3 and IL-18 mRNA expression in vWAT and liver tissue of NAFLD patients *vs.* controls. **C** In vWAT NLRP3 mRNA expression did not differ between patients with NAFLD and controls. **D** NLRP3 mRNA expression in liver tissue from patients was significantly downregulated compared to controls. Neither vWAT (e) nor liver tissue (f) revealed significant differences of IL-18 mRNA expression between patients and controls. We next determined serum concentrations of the cytokines pro-IL-1β/IL-1β and IL-18, which are released upon NLRP3-inflammasome activation. However, results have to be considered with caution since detectable serum concentrations were present only in 27 patients for pro-IL-1β and in 11 patients for IL-1β. Still the hepatic IL-1β mRNA concentration and its serum-borne protein were highly correlated (n = 7; **G**) as well as serum concentrations of pro-IL-1β and IL-1β (n = 7; **H**). (i) Serum IL-18 showed a positive correlation with the expression of RIPK3 mRNA in the liver (n = 42). There were no

further correlations between these interleukins with any other parameters tested. (j) Males patients with NAFLD had significantly higher IL-1β serum concentrations (females: n = 17; males: n = 11) than women, and (k) there was a highly significant difference between patients with hepatocellular ballooning (n = 8) *vs.* those without ballooning (n = 3). Statistics: *: $p \geq 0.01$ to 0.05; **: $p \geq 0.001$ to 0.01; ***: $p < 0.001$/r: Pearson's correlation coefficient; r_s: Spearman's rank correlation coefficient.

levels of pro-IL (Figure 5g, h) and were significantly lower in patients with hepatocellular ballooning (Figure 5k). Serum concentrations of pro-IL-1β were significantly higher in male patients with NAFLD (Figure 5j), and inversely correlated to collagen deposition in vWAT (Supplementary Figure 1c).

In NAFLD, autophagy-related LC3 mRNA expression is significantly downregulated in vWAT, but significantly upregulated in the liver

The mRNA expressions of the autophagy-related proteins LC3, ATG5, and Beclin-1 were measured in vWAT and liver tissue. In addition, we quantified ATG5-positive cells in vWAT tissue by IHC. While LC3 mRNA expression was significantly downregulated in vWAT of NAFLD patients (Figure 6a), it was significantly upregulated in liver tissue of NAFLD patients compared to controls (Figure 6d). Neither mRNA of ATG5 nor Beclin-1 mRNAs differed significantly between patients and controls in vWAT or liver tissue (Figure 6b, c, e, f). Notably, strongly contrasted its downregulation in vWAT (Figure 6a). The LC3 and ATG5 mRNA expressions (but not those of Beclin-1) in vWAT of NAFLD patients were significantly correlated with M30 serum levels (Figure 6g, h, i). The number of ATG5-positive cells was significantly correlated with the degree of collagen deposition (Figure 6k) but not with the expression of collagen 1α mRNA (Figure 6j) in the vWAT of NAFLD patients. The expression of ATG5 mRNA was significantly correlated with collagen 1α mRNA expression in vWAT (Figure 6l).

Discussion

Fibrosis causes up to 45% of all deaths in industrialized countries. It results from a dysregulated wound healing response following tissue injury, can affect any organ, and covers a wide spectrum of manifestations that can develop towards chronic fibrosis and the induction and progression of cancer [37]. More advanced stages of fibrosis usually go along with chronic inflammation and tissue injury [38,39]. A possible contribution of adipose tissue fibrosis to NAFLD has not been investigated in humans, in depth. We here showed that the profibrotic deposition of extracellular matrix in the vWAT of morbidly obese patients with NAFLD (i)

increases with age; (ii) is sex-specific, with women displaying a greater degree of fibrosis than men; and (iii) occurs inversely to the presence of hypertrophic adipocytes as smaller adipocytes were correlated with more collagen deposition fibrosis.

WAT regulates energy homoeostasis and, by storing triglycerides, serves as a systemic energy reservoir [40]. Excess energy is managed by the increase of adipocytes in size (hypertrophy) and number (hyperplasia). Mature small adipocytes (<20 μm to <70 μm diameter) can expand into large (~70–120 μm) and very large adipocytes, reaching a maximum diameter of ~300 μm [41]. We earlier demonstrated that the occurrence of very large adipocytes correlates with increased inflammatory activity and the incidence of NAFLD, T2DM, and other metabolic disorders [42]. These findings were complemented by results of other groups showing that adipocyte hypertrophy goes along with dysregulated adipocyte differentiation, enlargement of lipid droplets, an impaired insulin response and glucose uptake, increased FFA secretion, abnormal adipocyte osmolarity sensors, increased release of proinflammatory cytokines, exacerbation of hypoxia, excessive collagen deposition, and decreased adiponectin secretion. All of these aspects contribute to the dysregulation of systemic energy metabolism in morbid obesity [41,43], which suggests that the increase in adipocyte size and the ratio of large to small adipocytes might accelerate the development of NAFLD and T2DM [43].

Our present study demonstrates that the degree of fibrosis in vWAT inversely correlated with BMI and the size of vWAT-resident adipocytes. Fibrosis was thus mainly detected in vWAT areas populated with smaller adipocytes. Earlier findings already indicated that fibrosis limits the hypertrophic and excessive expansion of adipocytes [42,44–46]. As reviewed by Sun *et al.*, the results of multi-variate analyses in morbid obesity suggest that visceral fibrosis may limit adipocyte size whereby positively impacting circulating triglyceride levels. Visceral fibrogenesis might be induced as an adaptive mechanism mitigating negative effects resulting from hypoxia in rapidly expanding adipose tissue [47]. These findings are in line with our own observations.

The hypothesis of protective vWAT fibrosis is further supported by an inverse correlation of collagen deposition in vWAT and BMI of morbidly obese patients (Figure 1e). The systemic concentration of
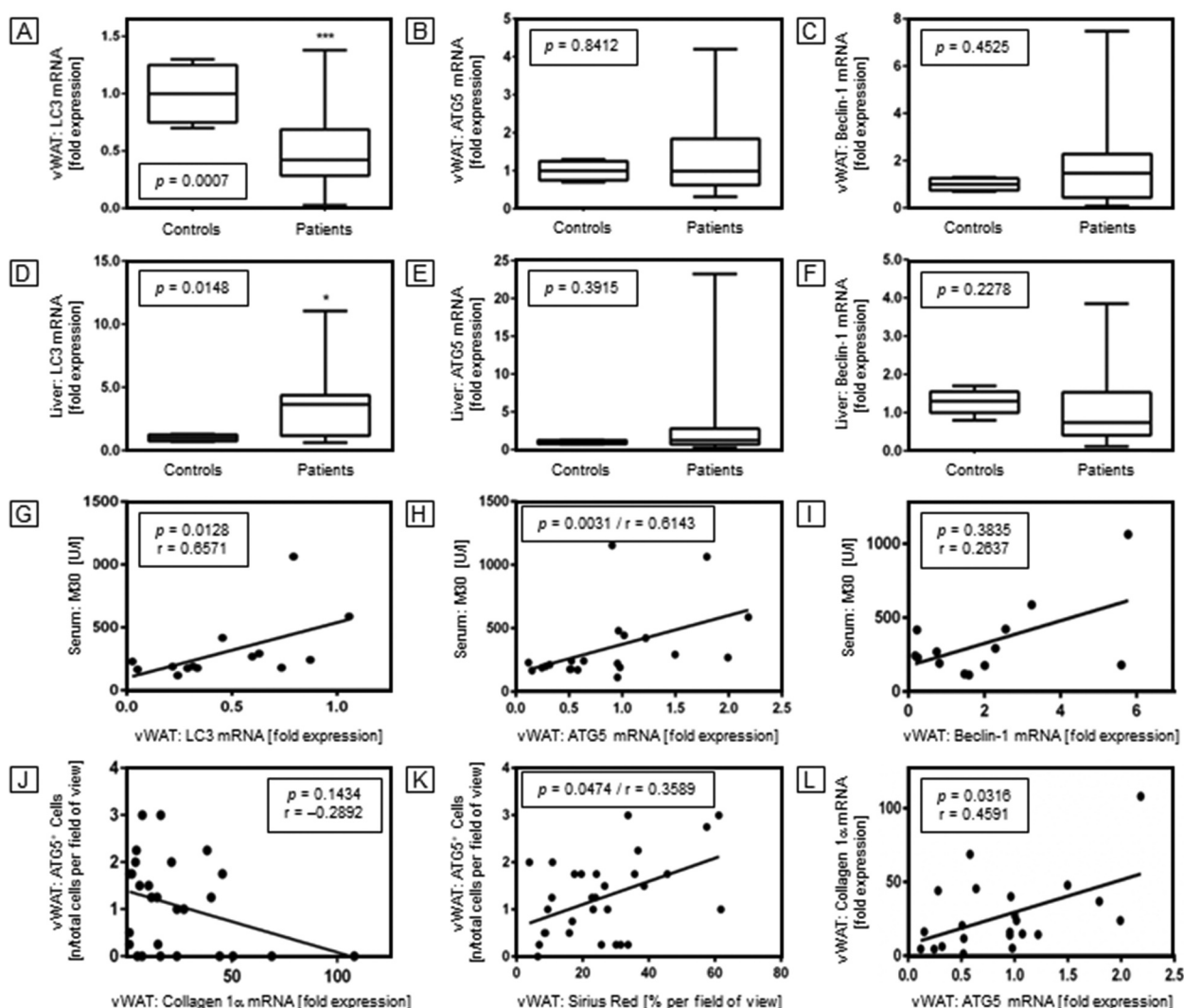
Figure 6. LC3 mRNA is expression is reduced in vWAT of patients with NAFLD and correlated to serum M30. A–C mRNA expressions of autophagy-related genes LC3, ATG5, and Beclin-1 in vWAT of NAFLD patients compared to controls. A LC3 mRNA expression was significantly reduced in the patients. B and C In contrast, neither the ATG5 nor the Beclin-1 mRNA expressions exhibited significant differences between patients and controls. D–F mRNA expressions of autophagy-related LC3, ATG5, and Beclin-1 in liver tissue of NAFLD patients compared to controls. D Significantly upregulated expression of LC3 mRNA in patients' liver tissue stood in stark contrast to the findings in vWAT. E and F Neither the ATG5 nor the Beclin-1 mRNA expressions differed significantly between the groups. G–I Correlations between the levels of mRNA expressions of LC3, ATG5, and Beclin in vWAT with the soluble apoptosis-related cell death marker M30 in NAFLD patients. G and H Statistically significant correlations were found both for the LC3 (n = 14) and the ATG5 (n = 13) mRNA expressions with M30 serum levels. I The correlation between Beclin-1 mRNA expression and M30 was not statistically significant (n = 13). J–L Correlations between collagen 1α mRNA expression or collagen deposition, respectively, with ATG5-positive cells, and correlation between ATG5 and collagen 1α mRNA expressions in vWAT of NAFLD patients. J Collagen 1α mRNA expression did not correlate with the presence of ATG5-positive cells (n = 27). K Collagen deposition correlated positively with the number of ATG5-positive cells (n = 29). L Likewise, the expression of ATG5 mRNA statistically significantly correlated with collagen 1α mRNA expression in the vWAT of NAFLD patients (n = 22). Statistics: *: $p \geq 0.01$ to 0.05; **: $p \geq 0.001$ to 0.01; ***: $p < 0.001$/r: Pearson's correlation coefficient.

adiponectin decreases in obesity [22,23]. During the development of liver fibrosis adiponectin serum concentrations increase again [24], which is in line with our finding that increased fibrosis in vWAT is associated with increased serum adiponectin levels. We detected significantly reduced adiponectin levels in the sera of NASH patients compared to those with NAFL

(Figure 2e); this confirms the findings by Finelli et al. who reported lower adiponectin concentrations in NASH correlating with a risk of severe disease progression [48]. Because of the absence of sex-specific differences, adiponectin may be considered a potential sex-independent marker for evaluating the severity and progression of NAFLD.

Serum concentrations of the apoptotic cell death marker M30 raised proportionally to the increase of fibrosis in the vWAT of NAFLD patients (Figure 3a), which was not the case for the M65 marker reflecting both apoptosis and necrosis (Figure 3b). Unlike in patients with other chronic liver diseases, such as hepatitis B [49], morbidly obese patients with NAFLD did not exhibit a correlation between serum M30 or M65 with collagen deposition in liver tissue. Apart from fibrosis M30 was correlated to expressions of the autophagy-related mRNAs for LC3, ATG5, and Beclin 1 in vWAT (Figure 6g-i). Autophagy is primarily a process of tissue maintenance, though uncontrolled autophagy may lead to cell death. Hence, autophagy may account for at least a portion of the increased cellular death rate found in vWAT of patients with NAFLD [50]. However, the here presented mRNA expressions cannot reflect functional activation of autophagic flux. To reliably quantify the contribution of autophagy to vWAT cell death, further analyses would be required.

The high-mobility group protein, HMGB1, serves as a (co-)transcription factor and as a chemoattractant, and elevated serum levels of HMGB1 can signify severity of a pathological condition, especially, related to necrotic cell death [51–53]. Intranuclearly, it enhances the expression of certain genes by increasing access to transcription factors [54]. To our knowledge, we here for the first time investigated the expression of HMGB1 in tissues from NAFLD patients. In mouse models of NAFLD and NASH, the expression of HMGB1 had always been found to be consistently upregulated in hepatocytes [55]. Surprisingly, we now found the exact opposite in both human vWAT and liver tissue in NAFLD (Figure 4a, b). If independently confirmed, these findings would imply that none of the present NAFLD mouse models mirrors HMGB1 expression in human hepatocytes in NAFLD.

There are a few limitations to our present study: First, we here focus on NAFLD patients with morbid obesity only; it thus remains to be clarified whether our findings are also representative for less obese patients and for the processes in vWAT in general. The retrospective nature of the dataset is associated with incomplete data, which limited statistical robustness in some analyses. This also implies that impact of medication could not be assessed, as detailed medication of individual patients was unknown. However, for all patients included liver histology was available, with fibrosis and NAS score as hard reference points for all analyses. Second, our study has shown that fibrosing in vWAT does not correlate with upregulated collagen 1α mRNA expression. Further studies should investigate (i) whether other collagen types are involved in vWAT fibrosis; (ii) whether matrix metalloproteinases and/or their specific endogenous inhibitors influence fibrosis extent in vWAT; and (iii) which cell type is responsible for extracellular collagen deposition in vWAT. Third, more in-depth examinations regarding the cell death modes are required to analyse, which pathways are actually activated in vWAT in human NAFLD. According to our results, the pathology of NAFLD is not dominated by one single pathway of regulated cell death, but rather presents as an interplay between different mechanisms both in vWAT and liver. Another limitation is the relatively low number of controls, which might also impair statistical robustness in comparisons between NAFLD patients and controls.

In summary, we demonstrated that collagen deposition in vWAT of morbidly obese patients with NAFLD inversely correlates with BMI and adipocyte size, suggesting a potentially protective effect against excessive adipocyte hypertrophy. In parallel, extent of vWAT fibrosis was correlated to liver fibrosis, serum M30 as surrogate marker for endothelial apoptosis, and vWAT ATG5-positive cells indicating a complex interplay of vWAT and liver fibrogenesis on the one hand, and cell death in these tissues on the other hand. We believe that our findings in human vWAT and liver samples suggest that vWAT fibrosis and different cell death modes or inflammatory pathways may influence NAFLD and possible progression to NASH.

Patients, materials and methods

Ethics

The study protocol conformed to the Declaration of Helsinki revised 2008. It was approved by the Ethics Committee (Institutional Review Board) of the Medical Faculty of the University Duisburg-Essen, Germany (file number: 09–4252).

Patients and surgical tissue sampling

The recruited patients were undergoing BAS at the Department of General and Visceral Surgery at Alfried Krupp Hospital (Essen, Germany). All patients met the criteria for surgical weight loss therapy established by the NIH consensus conference [56], i.e., age >18 yrs, body-mass index (BMI) ≥40 kg/m^2 or ≥35 kg/m^2 with co-morbidities (i.e., hypertension, dyslipidemia, and hyperglycaemia), failure of medical weight loss, absence of medical or psychological contraindications for BAS, and evaluation by a multi-disciplinary team of medical, nutrition, psychiatry, and surgical specialists. Patients received a single lesson of dietary

and activity counselling 6 months prior BAS. No calorie restriction was imposed during this time, weight change prior BAS was not recorded. Patients were educated about intraoperative risks of wedge liver and vWAT biopsy and provided written informed consent. BAS was carried out laparoscopically as described before [57]. Briefly, operations were either performed as Roux-en-Y gastric bypass, sleeve gastrectomy, or gastric banding according to the surgeons' decision. Wedge liver biopsies and samples of vWAT adjacent to the liver towards the median plane were obtained upon laparoscopic intervention. Intraoperatively, the excision of liver biopsies and vWAT was followed by appropriate coagulation; vWAT was sampled by ultrasound dissection during surgery. In addition, the provision of anthropometric patient data and routine laboratory parameters was ensured.

We excluded patients aged ≤18 or >65 years with liver pathologies other than NAFLD, history of organ transplantation, history of malignancy within the previous 5 years, alcohol abuse (women: >10 g/day; men: >20 g/day), drug abuse within the previous year, autoimmune or genetic disorders, therapy with immunosuppressive or hepatotoxic agents, or documented other known causes of secondary fatty liver diseases (e.g., viral hepatitides, toxic liver diseases, and/or metabolic liver diseases). A cohort of 84 patients (63 females; 21 males/age range: 46–84 years) complying with these criteria was identified. For patients' characteristics, see Table 1.

Control samples

Healthy liver tissue, vWAT and serum samples were collected from different sources of non-obese and disease-free individuals. The sample size of serum controls was n = 14 in total, with eight women, four men, and two persons of unknown sex. vWAT was sampled from four females, one male, and two patients of unknown sex during non-BAS abdominal surgery. Wedge liver biopsies for healthy liver tissue were obtained from four female and three male brain-dead liver transplant donors. No further information is available on these individuals. In the latter cases, written permission from the next of kin was obtained.

Sample preparation and general histology

Liver tissue samples were split and immediately transferred into 4% paraformaldehyde and RNAlater (MDL No.: MFCD03453003; Merck, Darmstadt, Germany). Serial 5-μm sections of paraffin embedded liver tissue

were stained with haematoxylin/eosin and an experienced pathologist (H.A. Baba) determined the NAFLD activity score (NAS) [58]. For the present analysis, a NAS of 1–4 was classified as NAFL, and a NAS of ≥5 as NASH.

vWAT was also fixed in paraffin and 5-μm sections were prepared. Mean adipocyte diameters were calculated from >50 individual measurements per sample as described before [42]. Each sample was scored in three independent fields of vision and by two independent investigators (M. Schlattjan, A.-S. Leven). Discordant results were discussed and jointly re-evaluated using a conference microscope. Sections of vWAT and liver tissue were assessed by Sirius Red staining for collagen indicating fibrosis.

Immunohistochemistry (IHC) for ATG5

Briefly, samples were dewaxed by xylene and rehydrated with a descending concentration series of ethanol (EtOH)–water mixtures (i.e., 100% EtOH: 0% H_2O → 90% EtOH: 10% H_2O → 70% EtOH: 30% H_2O → 50% EtOH: 50% H_2O for 5 min, each). Samples were then incubated for 10 min in PBS. ATG5 binding sites were exposed by incubation with proteinase K for 10 min at RT. Next, samples were washed twice with 0.1% PBS/Tween, blocked with 3% BSA solution for 40 min, and primary anti-ATG5 rabbit polyclonal to APG5L/ATG5 (Cat. No.: ab228668; Abcam plc., Cambridge, UK) was applied at 1:200 in PBS for 1 h at RT. Samples were washed three times for 5 min with PBS and incubated with Alexa Fluor 488-conjugated highly cross-adsorbed secondary donkey anti-rabbit IgG (H + L) (Cat. No.: A32790; ThermoFisher Scientific, Darmstadt, Germany). After another wash for 5 min in PBS, the samples were covered with ProLong Gold Antifade Mountant plus DAPI (Cat. No. P36931; ThermoFisher Scientific). Data were evaluated quantitatively for ATG5-positive and -negative cells using the open-source program ImageJ and the CellCounter plugin, and quotients of ATG5-positive cells per total counted cells per field of view were determined.

Quantitative real-time polymerase chain reaction (qRT-PCR)

Isolation of mRNA from tissue and qRT-PCR were performed as described before [27]. Briefly, vWAT and liver tissue were homogenized in TRIZOL (Invitrogen, Karlsruhe, Germany) using a blade homogenizer (IKA, Staufen, Germany). Total RNA was isolated with the RNeasy Mini Kit (Cat. Nos. 74,104 & 74,106; Qiagen, Hilden, Germany), and the mRNA purity and concentration were determined photometrically. Samples of 2 mg RNA, each, were then dissolved

in 100 ml of RNase-free water, and reverse transcription was performed using the QuantiTect Reverse Transcription Kit (Cat. No. 205,311; Qiagen). Levels of mRNA expression related to gene products of (i) fibrosis (collagen 1α); (ii) necrosis (HMGB1); (iii) necroptosis (RIPK3); (iv) pyroptosis (NLRP3; IL-18); and (v) autophagy-dependent cell death (ATG5; LC3; Beclin-1) were then determined by qRT-PCR using hypoxanthine phosphoribosyltransferase 1 as a reference gene (cf. Table 2). qRT-PCRs of the cDNAs were performed using an iCycler iQ 3.1 thermal cycler (Bio-Rad, Hercules, CA, USA) with real-time detection system software 3.0a and GenEx software (Bio-Rad) in 30-μl reactions containing 15 μl QuantiTect SYBR Green master mix (Cat. No. 204,141; Qiagen), 2 μl cDNA, 1 μl forward primer, 1 μl reverse primer (at 10 pmol/ml, each), and 11 μl distilled water (primers from Eurofins Genomics, Ebersberg, Germany). Amplification was performed for 15 min at 95°C, followed by 40 cycles of 30 s at 95°C, 30 s at 55°C, and 30 s at 72°C. Melting-curve data were collected from 95°C to 55°C, at – 0.5°C steps for 10 s, each. Relative gene expressions vs. healthy controls were calculated from the threshold cycles in relation to the reference gene and expressed as fold-expression.

Table 2. Alphabetical list of human primers used in this study.

Primer[a]	Primer sequences (5′ to 3′)	T_a
ATG5		
F ATG_5	5′-TCA.AGT.TCA.GCT.CTT.CCT.TGG-3′	57.9
R ATG_5	5′-GCA.TCC.TTA.GAT.GGA.CAG.TGC-3′	59.8
Beclin-1		
F Beclin_1	5′-TCA.GCT.CAA.CGT.CAC.TGA.AAA-3′	55.9
R Beclin_1	5′-GCG.TCT.CCT.TTA.GCT.CCA.TC-3′	59.4
Collagen		
F Collagen	5′-AAC.AGC.CGC.TTC.ACC.TAC.AG-3′	59.4
R Collagen	5′-GGA.GGT.CTT.GGT.GGT.TTF.GT-3′	57.3
HMGB1		
F HMGB1	5′-AGA.GCG.GAG.AGA.GTG.AGG.AG-3′	61.4
R HMGB1	5′-ATG.TTT.AGT.TAT.TTT.TCC.TCA.GCG.A-3′	56.4
HPRT1		
F HPRT	5′-CTT.GCG.ACC.TTG.ACC.ATC.TT-3′	57.3
R HPRT	5′-GAC.CAG.TCA.ACA.GGG.GAC.AT-3′	59.4
IL-18		
F IL-18	5′-CGC.TTT.ACT.TTA.TAG.AAA.ACC.TGG.A-3′	58.1
R IL-18	5′-GAG.GCC.GAT.TTC.CTT.GGT.CA-3′	59.4
LC3		
F LC_3	5′-CGA.CCG.CTG.TAA.GGA.GGT.A-3′	58.8
R LC_3	5′-CAG.CTG.CTT.CTC.ACC.CTT.GT-3′	59.4
NLRP3		
F NLRP3	5′-AGA.AGC.TCT.GGT.TGG.TCA.GC-3′	59.4
R NLRP3	5′-CAA.GGC.ATT.CTC.CCC.CAC.AT-3′	59.4
RIPK3		
F RIPK3	5′- TGG.CCC.CAG.AAC.TGT.TTG.TT −3′	60.0
R RIPK3	5′- GGA.TCC.CGA.AGC.TGT.AGA.CG −3′	60.0

ATG5 autophagy related 5, *HMGB1* high-mobility group box 1 protein, *HPRT1* hypoxanthine phosphoribosyltransferase 1, *IL-18* interleukin 18, *LC3* microtubule-associated proteins 1A/1B light chain 3B, *NLRP3* nucleotide-binding oligomerization domain, leucine rich repeat and pyrin domain containing 3, *RIPK3* receptor-interacting serine/threonine-protein kinase 3, T_a annealing temperature
[a]F: forward primer, R: reverse primer.

Terminal deoxynucleotidyl transferase-mediated dUTP nick-end labelling (TUNEL)

DNA fragmentation in vWAT due to apoptosis and/or of cells that suffered severe DNA damage was detected by TUNEL as described before [57,59]. Briefly, 5-μm paraffin tissue sections were analysed by the TUNEL assay (Cat. No. Cat. No. 11,684,795,910; Roche, Mannheim, Germany), which enzymatically labels free 3′-OH ends of damaged DNA with a fluorophore-conjugated nucleotide. Ten high-power fields per patient were quantified for fluorescent nuclei at λ_{EX} = 380 nm and λ_{EM} = 430 nm, using an inverted laser scanning confocal microscope (LSM 510; Carl Zeiss Micro-Imaging, Göttingen, Germany) equipped with a × 40 NA 1.4 lens and LSM 510 imaging software. Data are expressed as numbers of TUNEL-positive cells/10 high-power fields.

Detection of serum marker and interleukin concentrations by enzyme-linked immunosorbent assay (ELISA)

To measure the concentrations of the cytokeratin epitopes M30 and M65 and the interleukines pro-IL-1β, IL-1β, and IL-18 commercially available ELISA kits were employed. Briefly, patients' sera were analysed for M30 and M65 using the M30-Apoptosense (Prod. No. 10010) and M65 (Prod. No. 10020) ELISA kits (Peviva, Bromma, Sweden) according to the manufacturers' instructions and as described before [27]. The neo-epitope M30 exposed upon caspase 3-dependent cleavage of cytokeratin 18 is a marker for apoptosis, while M65 identifies both M30 and intact cytokeratin 18 and, therefore, indicates both apoptosis and necrosis.

Human interleukin serum concentrations were determined with commercial ELISA kits for pro-IL-1β (SKU: HUFI02788; AssayGenie, Dublin, Ireland), IL-1β (Cat. No. BMS224-2; Invitrogen via ThermoFisher Scientific) and IL-18 (Cat. No.: BMS267-2; Invitrogen via ThermoFisher Scientific), according to the manufacturers' instructions. Briefly, 50 μl of patients' sera were admixed with 50 μl of sample diluent provided with the respective kits and incubated in the pre-coated plates for the times indicated. Detection was performed via biotin-labelled antibodies and peroxidase-conjugated streptavidin. Colour development of 3,3′,5,5′-tetramethyl-benzidine was stopped by adding acid solution and measured at 450 nm (Multiskan RC, Labsystems Diagnostics, Vantaa, Finland). Standard curves ranged from 31.3 to 2000 pg/ml for pro-IL-1β, from 3.9 to 250 pg/ml for IL-1β, and from 78 to

5000 pg/ml for IL-18. Concentrations were calculated from the respective standard curves using MS Excel 2019.

Data analyses and statistics

Analyses were performed using Microsoft Office Excel 2013 (Microsoft, Redmond, WA, USA) and Prism versions 6.0 and 9.0 for Windows (GraphPad Software, La Jolla, CA, USA). Differences between two groups of data with a non-normal distribution were compared by Mann–Whitney test, and normally distributed data were compared with unpaired Student's t-test, with Welch correction in case of significantly different variances. Differences between ≥3 groups were assessed by ANOVA. The significance level was set at α = 5% for all comparisons. Results of group comparisons are presented as box and whisker plots with median, 25% and 75 quartiles (box), and range (whiskers).

To assess correlation of two parametrically distributed variables, Pearson's correlation coefficient (r) was applied. Correlations with at least one non-parametrically distributed variable were determined by Spearman's rank correlation coefficient (r_s).

Acknowledgments

Disclosure statement

No potential conflict of interest was reported by the authors.

Data availability statement for publicly available data sharing policy

The full dataset is available on reasonable request to the corresponding author as patient-level data are subject to German data protection laws.

Declarations and ethics statements

The study protocol conformed to the Declaration of Helsinki revised 2008. It was approved by the Ethics Committee (Institutional Review Board) of the Medical Faculty of the University Duisburg-Essen, Germany (file number: 09-4252).

Author contributions

JPS and AC conceived and designed the study. ASL, JMS, TS, MN, TB, HAB and MKÖ obtained and processed tissue as well as performed histological investigations and experiments. RKG, JPS and ASL analyzed data. RKG, ASL and JPS created figures and tables. RKG and ASL wrote the manuscript. AC supervised the project and critically read the manuscript.

ORCID

Anna-Sophia Leven http://orcid.org/0000-0002-5247-1125
Robert K. Gieseler http://orcid.org/0000-0002-3064-8516
Martin Schlattjan http://orcid.org/0000-0001-6639-5568
Thomas Schreiter http://orcid.org/0000-0002-2956-5393
Marco Niedergethmann http://orcid.org/0000-0003-1803-4973
Theodor Baars http://orcid.org/0000-0002-1862-6461
Hideo A. Baba http://orcid.org/0000-0002-1750-5318
Mustafa K. Özçürümez http://orcid.org/0000-0002-4360-5005
Jan-Peter Sowa http://orcid.org/0000-0003-2943-0015
Ali Canbay http://orcid.org/0000-0001-6069-7899

References

[1] Younossi ZM, Koenig AB, Abdelatif D, et al. Global epidemiology of nonalcoholic fatty liver disease-Meta-analytic assessment of prevalence, incidence, and outcomes. Hepatology 2016 Jul;64(1):73–84.
[2] Sayiner M, Koenig A, Henry L, et al. Epidemiology of Nonalcoholic Fatty Liver Disease and Nonalcoholic Steatohepatitis in the United States and the Rest of the World. Clin Liver Dis. 2016 May;20(2):205–214.
[3] Long MT, Gandhi S, Loomba R. Advances in non-invasive biomarkers for the diagnosis and monitoring of non-alcoholic fatty liver disease. Metabolism 2020 Oct;111S:154259.
[4] Mitra S, De A, Chowdhury A. Epidemiology of non-alcoholic and alcoholic fatty liver diseases. 2020; Transl Gastroenterol Hepatol. 5:16.
[5] Mazzolini G, Sowa J-P, Atorrasagasti C, et al. Significance of Simple Steatosis: an Update on the Clinical and Molecular Evidence. Cells 2020 Nov;9 (11):2458.
[6] Younossi ZM, Tampi R, Priyadarshini M, et al. Burden of Illness and Economic Model for Patients With Nonalcoholic Steatohepatitis in the United States. Hepatology. 2019;69(2):564–572.
[7] Brunt EM, Wong VW-S, Nobili V, et al. Nonalcoholic fatty liver disease. Nat Rev Dis Primers. 2015 Dec;17 (1):15080.
[8] Friedman SL. Liver fibrosis – from bench to bedside. J Hepatol. 2003;38(Suppl 1):S38–53.
[9] Bataller R, Brenner DA. Liver fibrosis. J Clin Invest. 2005 Feb 1;115(2):209–218.
[10] Wynn TA. Integrating mechanisms of pulmonary fibrosis. J Exp Med. 2011 Jul 4;208(7):1339–1350.
[11] Angulo P, Kleiner DE, Dam-Larsen S, et al. Liver Fibrosis, but No Other Histologic Features, Is Associated With Long-term Outcomes of Patients With Nonalcoholic Fatty Liver Disease. Gastroenterology. 2015 Aug;149(2):389–397.e10.
[12] Manka PP, Kaya E, Canbay A, et al.Review of the Epidemiology, Pathophysiology, and Efficacy of

Anti-diabetic Drugs Used in the Treatment of Nonalcoholic Fatty Liver Disease.Dig Dis Sci [Internet]. 2021 Aug 19 [cited 2021 Sep 13]; Available from:.10.1007/s10620-021-07206-9.

[13] Alberti KGMM, Eckel RH, Grundy SM, et al. Harmonizing the metabolic syndrome: a joint interim statement of the International Diabetes Federation Task Force on Epidemiology and Prevention; National Heart, Lung, and Blood Institute; American Heart Association; World Heart Federation; International Atherosclerosis Society; and International Association for the Study of Obesity. Circulation. 2009 Oct 20;120(16):1640–1645.

[14] Grundy SM, Cleeman JI, Daniels SR, et al. Diagnosis and management of the metabolic syndrome: an American Heart Association/National Heart, Lung, and Blood Institute scientific statement: executive Summary. Crit Pathw Cardiol. 2005 Dec;4(4):198–203.

[15] Nilsson PM, Tuomilehto J, Rydén L. The metabolic syndrome - What is it and how should it be managed? Eur J Prev Cardiol. 2019 Dec;26(2_suppl):33–46.

[16] Bugianesi E, McCullough AJ, Marchesini G. Insulin resistance: a metabolic pathway to chronic liver disease. Hepatology 2005 Nov;42(5):987–1000.

[17] Watt MJ, Miotto PM, De Nardo W, et al. The Liver as an Endocrine Organ-Linking NAFLD and Insulin Resistance. Endocr Rev. 2019 Oct 1;40(5):1367–1393.

[18] Du Plessis J, Van Pelt J, Korf H, et al. Association of Adipose Tissue Inflammation With Histologic Severity of Nonalcoholic Fatty Liver Disease. Gastroenterology. 2015 Sep;149(3):635–648.e14.

[19] Chung GE, Kim D, Kwark MS, et al. Visceral adipose tissue area as an independent risk factor for elevated liver enzyme in nonalcoholic fatty liver disease. Medicine (Baltimore). 2015 Mar;94(9):e573.

[20] Kucukoglu O, Sowa J-P, Mazzolini GD, et al. Hepatokines and adipokines in NASH-related hepatocellular carcinoma. J Hepatol. 2021 Feb;74(2):442–457.

[21] Wree A, Kahraman A, Gerken G, et al. Obesity affects the liver - the link between adipocytes and hepatocytes. Digestion. 2011;83(1–2):124–133.

[22] Díez JJ, Iglesias P. The role of the novel adipocyte-derived protein adiponectin in human disease: an update. Mini Rev Med Chem. 2010 Aug;10(9):856–869.

[23] Yadav A, Kataria MA, Saini V, et al. Role of leptin and adiponectin in insulin resistance. Clin Chim Acta. 2013 Feb ;18(417):80–84.

[24] Ding X, Saxena NK, Lin S, et al. The Roles of Leptin and Adiponectin. Am J Pathol. 2005 Jun;166(6):1655–1679.

[25] Mazzolini G, Sowa J-P CA. Cell death mechanisms in human chronic liver diseases: a far cry from clinical applicability. Clin Sci. 2016 Dec 1;130(23):2121–2138.

[26] Galluzzi L, Vitale I, Aaronson SA, et al. Molecular mechanisms of cell death: recommendations of the Nomenclature Committee on Cell Death 2018. Cell Death Differ. 2018 Mar;25(3):486–541.

[27] Bechmann LP, Jochum C, and Kocabayoglu P, et al. Cytokeratin 18-based modification of the MELD score improves prediction of spontaneous survival after acute liver injury. J Hepatol. 2010 Oct ;53 (4):639–647.cited 2010

[28] Scaffidi P, Misteli T, Bianchi ME. Release of chromatin protein HMGB1 by necrotic cells triggers inflammation. Nature. 2002 Jul 11;418(6894):191–195.

[29] Degterev A, Huang Z, Boyce M, et al. Chemical inhibitor of nonapoptotic cell death with therapeutic potential for ischemic brain injury. Nature Chemical Biology. 2005 Jul;1(2):112–119.

[30] Ni H-M, Chao X, Kaseff J, et al. Receptor-Interacting Serine/Threonine-Protein Kinase 3 (RIPK3)-Mixed Lineage Kinase Domain-Like Protein (MLKL)-Mediated Necroptosis Contributes to Ischemia-Reperfusion Injury of Steatotic Livers. Am J Pathol. 2019 Jul;189(7):1363–1374.

[31] Roedig J, Kowald L, Juretschke T, et al. USP22 controls necroptosis by regulating receptor-interacting protein kinase 3 ubiquitination. EMBO Rep. 2021 Feb 3;22(2): e50163.

[32] Hou L, Zhang Z, Yang L, et al. NLRP3 inflammasome priming and activation in cholestatic liver injury via the sphingosine 1-phosphate/S1P receptor 2/Gα(12/13)/MAPK signaling pathway. J Mol Med (Berl). 2021 Feb;99(2):273–288.

[33] Zhang X-W, Zhou J-C, Peng D, et al. Disrupting the TRIB3-SQSTM1 interaction reduces liver fibrosis by restoring autophagy and suppressing exosome-mediated HSC activation. Autophagy. 2020 May;16(5):782–796.

[34] Klionsky DJ, Abdelmohsen K, Abe A, et al. Guidelines for the use and interpretation of assays for monitoring autophagy (3rd edition). Autophagy. 2016;12(1):1–222.

[35] Tao -L-L, Zhai Y-Z, Ding D, et al. The role of C/EBP-α expression in human liver and liver fibrosis and its relationship with autophagy. Int J Clin Exp Pathol. 2015;8(10):13102–13107.

[36] He Y, Ao N, Yang J, et al. The preventive effect of liraglutide on the lipotoxic liver injury via increasing autophagy. Ann Hepatol. 2020 Feb;19(1): 44–52.

[37] Henderson NC, Rieder F, Wynn TA. Fibrosis: from mechanisms to medicines. Nature 2020 Nov;587 (7835):555–566.

[38] Rybinski B, Franco-Barraza J, Cukierman E. The wound healing, chronic fibrosis, and cancer progression triad. Physiol Genomics. 2014 Apr 1;46(7):223–244.

[39] Gamaev L, Mizrahi L, Friehmann T, et al. The pro-oncogenic effect of the lncRNA H19 in the development of chronic inflammation-mediated hepatocellular carcinoma. Oncogene. 2021 Jan;40(1):127–139.

[40] Choe SS, Huh JY, Hwang IJ, et al. Adipose Tissue Remodeling: its Role in Energy Metabolism and Metabolic Disorders. Front Endocrinol (Lausanne). 2016;7:30.

[41] Stenkula KG, Erlanson-Albertsson C. Adipose cell size: importance in health and disease. Am J Physiol Regul Integr Comp Physiol. 2018 Aug 1;315(2):R284–95.

[42] Wree A, Schlattjan M, Bechmann LP, et al. Adipocyte cell size, free fatty acids and apolipoproteins are associated with non-alcoholic liver injury progression in

severely obese patients. Metab Clin Exp. 2014 Dec;63 (12):1542–1552.

[43] Liu F, He J, Wang H, et al. a Critical Factor in Regulation of Human Metabolic Diseases and Adipose Tissue Dysfunction. Obes Surg. 2020 Dec;30 (12):5086–5100.

[44] Divoux A, Tordjman J, Lacasa D, et al. Fibrosis in Human Adipose Tissue: composition, Distribution, and Link With Lipid Metabolism and Fat Mass Loss. Diabetes 2010 Nov;59(11):2817–2825.

[45] Muir LA, Neeley CK, Meyer KA, et al. Adipose tissue fibrosis, hypertrophy, and hyperplasia: correlations with diabetes in human obesity. Obesity (Silver Spring). 2016 Mar;24(3):597–605.

[46] Skurk T, Alberti-Huber C, Herder C, et al. Relationship between adipocyte size and adipokine expression and secretion. J Clin Endocrinol Metab. 2007 Mar;92 (3):1023–1033.

[47] Sun K, Tordjman J, Clément K, et al. Fibrosis and adipose tissue dysfunction. Cell Metab. 2013 Oct 1;18 (4):470–477.

[48] Finelli C, Tarantino G. What is the role of adiponectin in obesity related non-alcoholic fatty liver disease? World J Gastroenterol. 2013 Feb 14;19(6):802–812.

[49] Wei X, Wei H, Lin W, et al. Cell death biomarker M65 is a useful indicator of liver inflammation and fibrosis in chronic hepatitis B: a cross-sectional study of diagnostic accuracy. Medicine (Baltimore). 2017 May;96(20):e6807.

[50] Maixner N, Kovsan J, Harman-Boehm I, et al. Autophagy in adipose tissue. Obes Facts. 2012;5(5):710–721.

[51] Kang R, Chen R, Zhang Q, et al. HMGB1 in Health and Disease. Mol Aspects Med. 2014;0:1–116.

[52] Luedde T, Kaplowitz N, Schwabe RF. Cell Death and Cell Death Responses in Liver Disease:</L> Mechanisms and Clinical Relevance. Gastroenterology. 2014 Oct;147(4):765–783.e4.

[53] Campana L, Bosurgi L, Rovere-Querini P. HMGB1: a two-headed signal regulating tumor progression and immunity. Curr Opin Immunol. 2008 Oct;20 (5):518–523.

[54] Lotze MT, Tracey KJ. High-mobility group box 1 protein (HMGB1): nuclear weapon in the immune arsenal. Nat Rev Immunol. 2005 Apr;5(4):331–342.

[55] Koyama Y, Brenner DA. Liver inflammation and fibrosis. J Clin Invest. 2017 Jan 3;127(1):55–64.

[56] Brolin RE. Update: NIH consensus conference. Gastrointestinal surgery for severe obesity. Nutrition. 1996;12(6):403–404. Jun.

[57] Kahraman A, Schlattjan M, Kocabayoglu P, et al. Major histocompatibility complex class I-related chains A and B (MIC A/B): a novel role in nonalcoholic steatohepatitis. Hepatology 2010 Jan;51(1):92–102.

[58] Kleiner DE, Brunt EM, Van Natta M, et al. Design and validation of a histological scoring system for nonalcoholic fatty liver disease. Hepatology 2005 Jun;41 (6):1313–1321.

[59] Natori S, Selzner M, Valentino KL, et al. Apoptosis of sinusoidal endothelial cells occurs during liver preservation injury by a caspase-dependent mechanism. Transplantation. 1999 Jul 15;68(1):89–96.